Journal of Materials Chemistry B

Accepted Manuscript

ROYAL SOCIETY OF CHEMISTRY

www.rsc.org/materialsB

Journal Name

RSCPublishing

ARTICLE

A Water Soluble Initiator Prepared through Host-Guest Chemical Interaction for Microfabrication of 3D Hydrogels via Two-Photon Polymerization

Jinfeng Xing*[a], Jinhao Liu[a], Tingbin Zhang[a], Ling Zhang[a], Meiling Zheng*[b], Xuanming Duan*[b, c]

Cite this: DOI: 10.1039/x0xx00000x

Received 00th January 2014,
Accepted 00th January 2014

DOI: 10.1039/x0xx00000x

www.rsc.org/

Hydrogels with precise 3D configuration (3D hydrogels) are required for a number of biomedical applications such as tissue engineering and drug delivery. Two-photon polymerization (TPP) is an advanced method to fabricate 3D hydrogels. However, TPP of 3D hydrogels has been challenged by the lack of TPP initiators with high efficiency in aqueous medium. In this study, a water soluble TPP initiator (**WI**) with high fabrication efficiency was prepared by combining hydrophobic 2, 7-bis(2-(4-pentaneoxy-phenyl)-vinyl)anthraquinone (**N**) with C_{2v} symmetrical structure and 2-hydroxypropyl-β-cyclodextrins through host-guest chemical interaction. Both one and two-photon optical properties of **WI** have been investigated. In aqueous medium, **WI** showed a two-photon absorption cross-section of around 200 GM at the wavelength of 780 nm which was much higher compared with that of commercial initiators. The threshold energy of TPP for the resin with **WI** as photoinitiator (the molar ratio of **N** in resin is 0.03%) was 8.6 mW. 3D hydrogels with woodpile microstructure were further fabricated by using an average power of 9.7 mW and a scanning speed of 30 μm s^{-1}.

Introduction

Two-photon absorption (TPA) as a third order nonlinear optical process is defined as the electronic excitation of a molecule induced by a simultaneous absorption of two photons with the same or different energy.[1-3] TPA has played important roles in two-photon laser scanning fluorescence microscopy,[4-6] three dimensional (3D) microfabrication,[7-10] 3D optical data storage,[11] optical power limiting[12] and photodynamic therapy.[13, 14] These applications take advantage of the fact that the TPA probability is quadratically proportional to the intensity of the incident light.[15] Among these applications, two-photon polymerization (TPP) microfabrication was particularly favored because it can create fully 3D structures with a spatial resolution beyond the optical diffraction limit.[16, 17] Generally, the materials used for TPP microfabrication include negative and positive photoresists. It has been reported that negative photoresists can be easily modified and combined with active components for added functionality in the microstructure compared with positive photoresists.[16] Acrylic oligomers and epoxy resins that can create structures with high aspect ratios are typical negative photoresist resins.[18-20] Notably, an efficient TPP photoinitiator is indispensable for negative photoresist. A large TPA cross section (δ_{TPA}) is the prerequisite for TPP initiator with high initiating efficiency, and it is influenced by donor and acceptor strength, conjugation length and planarity of the π center.[21, 22] However, only large δ_{TPA} itself may not guarantee the high initiating efficiency of TPP initiators, and low fluorescence quantum yield is another key parameter for TPP photoinitiators with high initiating efficiency.[23, 24]

Up to now, a series of initiators with high initiating efficiency has been designed and synthesized.[25-27] Our previous work has been focused on designing and synthesizing TPP initiators with C_{2v} symmetrical structure.[23, 24, 28] However, few TPP initiators are suitable for fabricating 3D hydrogels. It is known that 3D hydrogels is extremely important for a number of biomedical applications such as tissue engineering and drug delivery.[29, 30] At present, TPP microfabrication by using femtosecond laser is one of the most advanced technologies for fabricating ultra-precise structures at the cell scale.[31] Although 3D hydrogels fabricated via TPP have been reported, most of them were prepared in organic solvent.[32, 33] Jhaveri et al. succeeded in fabricating hydrogels via TPP in aqueous media. However, the threshold energy reached 20 mW.[34] Torgersen et al. fabricated 3D hydrogels in aqueous medium and the laser power of fabrication was high up to 60 mW.[35] The disadvantages of high energy threshold in TPP include two

aspects that the resolution of fabricated lines could decrease and the microstructure fabricated might be damaged.[17, 36]

Consequently, the crucial barrier for TPP microfabrication of 3D hydrogels is the lack of TPP initiators with high efficiency in aqueous medium. In this study, we provided a universal method to prepare water soluble TPP initiators with high efficiency by using host-guest chemical interaction and then 3D hydrogels can be fabricated via TPP in aqueous medium. In detail, we prepared a water soluble TPP initiator (**WI**) by combining novel hydrophobic 2, 7-bis(2-(4-pentaneoxy-phenyl)-vinyl)anthraquinone (**N**) with C_{2v} symmetrical structure and 2-hydroxypropyl-β-cyclodextrins (2-Hp-β-CDs) through host-guest chemical interaction. **N** (the synthetic route is outlined on Scheme1) was designed as a hydrophobic TPP initiator with high efficiency and prepared through wittig reaction according to our previous study.[23] The long alkyl chain can guarantee **N**'s excellent solubility in organic solvent to assemble with 2-Hp-β-CDs effectively. Both one and two-photon optical properties of **WI** have been investigated. 3D hydrogels were further prepared utilizing **WI** as the TPP initiator with low laser power.

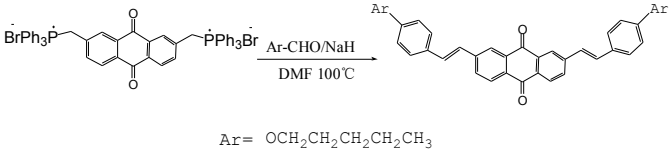

Scheme1. The synthetic route of **N**

Experiment

Materials

2,7-Bis-[(triphenylphosphonium bromide)-methyl]-anthraquinone in Scheme 1 was synthesized according to our previous report.[23] N-Bromosuccinimide (NBS), benzoyl peroxide (BPO), triphenylphosphine (PPh_3) and all of the solvent were obtained from Jiangtian Chemical Reagent Company. 4-methylphthalic anhydride was purchased from TCI Chemical Reagent Company. 4-n-pentyloxybenzaldehyde was purchased from Alfa Aesar Chemical Reagent Company and 2-Hydroxypropyl-β-cyclodextrins was purchased from Aladdin Chemical Reagent Company. Poly (ethylene glycol) diacrylate (PEGda) and 2-benzyl-2-(dimethylamino)-4'-morpholinobutyrophenone were purchased from Sigma-Aldrich Reagent Company.

Experimental

Synthesis of 2, 7-bis(2-(4-pentaneoxy-phenyl)-vinyl)anthraquinone (N): 2,7-Bis-[(triphenylphosphonium bromide)-methyl]-anthraquinone (1.61 g, 1.75 mmol) and 4-pentaneoxy-benzaldehyde (1.17 g, 6.08 mmol) were added to a two-neck flask containing absolute N,N-dimethylformamide (50 mL) under N_2 protection, and then NaH (0.25 g, 10.42 mmol) was added into the solution. The solution was kept at 100 °C for 20 h. Water (200 mL) was added slowly after the solution was cooled to room temperature. The formed precipitate was filtered, washed with ethanol (15 mL × 2), and recrystallized from a chloroform solution to get faint yellow powder (0.33 g, 31.96% yield). M. p. 209-211 °C. IR (KBr, cm^{-1}): 2930, 1667, 1593, 1509, 1323, 1260, 1026, 966, 815. ^1H NMR (500 MHz $CDCl_3$ δ(ppm)): 8.34 (s, 2H), 8.24 (d, *J*=8 Hz, 2H), 7.80 (d, *J*=8 Hz, 2H), 7.49 (d, *J*=8 Hz, 4H), 7.28 (t, *J*=16 Hz, 4H), 7.05 (d, *J*=16.5 Hz, 2H), 6.91 (d, *J*=8.5 Hz, 4H), 3.99 (t, 4H), 1.83 (m, 4H), 1.43 (m, 8H), 0.94 (t, 6H).

Preparation of N/2-Hp-β-CDs complex (WI): An orthogonal experiment was carried out to investigate the optimal condition of self-assembly by adjusting the influencing factors including temperature, the molar ratio of host and guest as well as the time of self-assembly. According to the orthogonal experiment, an optimal condition was determined. In detail, 2-Hp-β-CDs (262.3 mg, 0.17 mmol) were dissolved in water (50 mL) and **N** (5.8 mg, 0.01mmol) was dissolved in tetrahydrofuran (THF) (10 mL) at room temperature. The detailed assembly process is shown as follows: The solution of 2-Hp-β-CDs (5 mL) was added to test tube, and then **N** (1 mL) was added slowly and kept stirring at 50 °C for 12 h. After THF volatilized completely, the solution (4 mL) was freeze-dried and the lyophilized powder of **WI** was obtained.

Determination of UV-vis absorption and fluorescence spectra: UV-vis spectra were measured with a Diode Array UV-vis spectrophotometer. One-photon fluorescence spectra were measured with a Luminescence Spectrometer LS 50B using a Xenon lamp as a light source with the emission and excitation slit of 5 nm.

Determination of fluorescence quantum yield: Fluorescence quantum yield measurements were carried out using a luminescence spectrometer. The fluorescence quantum yield of samples in solutions were recorded by using coumarin 307 (Φ=0.58) as a reference in acetonitrile. **N** and **WI** were dissolved in $CHCl_3$ and deionized H_2O, respectively.

Determination of two-photon absorption cross-section: TPA cross-section (δ_{TPA}) was measured by using the two-photon fluorescence method with the standard fluorescein in NaOH aqueous solution (pH=13) according to the reference.[37] Two-photon excitation spectra were measured by using a mode-locked Ti: Sapphire laser excitation source. The laser provides a pulse of approximately 120 fs pulse width at a pulse repetition frequency of 80 MHz in the wavelength range of 710-890 nm. The pumping wavelengths were determined by a monochromator-charge coupled device system.

Two-photon polymerization processing: In this work, near-infrared Ti: sapphire femtosecond laser beam (120 fs, 80 MHz, 780 nm) was used to fabricate 3D hydrogels. The experimental setup for TPP microfabrication is shown in Scheme 2. The resins were made by mixing poly(ethylene glycol) diacrylate (PEGda)[38] as monomer, with **WI** as initiator in an aqueous medium and 2-benzyl-2-(dimethylamino)-4'-morpholinobutyrophenone as photosensitizer in a little DMF.

The laser beam was tightly focused by a 100 × oil immersion objective lens with a high numerical aperture (NA=1.45, Olympus). The focal point was focused on the liquid resin which was placed on a cover glass above the xyz-step motorized stage (P-563 3CL, Physik Instrumente) controlled by a computer. After fabrication, the unpolymerized resins were washed out with ethanol. The images of fabrication structures were observed using a field-emission scanning electron microscope.

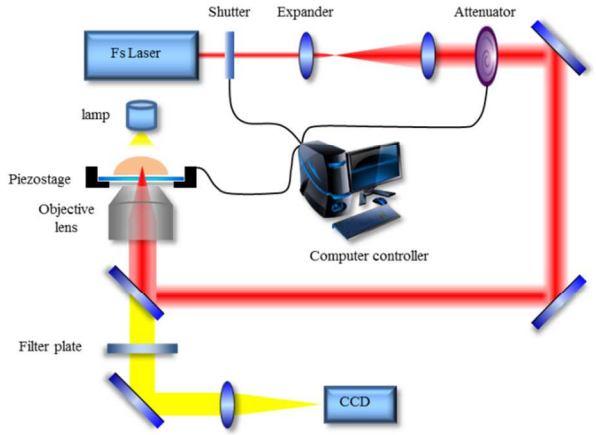

Scheme 2. Experimental setup for TPP microfabrication.

Results and Discussion

Linear optical properties

The UV-vis absorption and fluorescence spectra of **N** and **WI** are shown in Fig. 1. **N** has two absorption peaks at 443 nm and 328 nm. The absorption peak at 443 nm corresponds to electronic transition from the ground state to the intramolecular charge transfer (ICT) state. As shown in Fig. 1, the absorption peak at 328 nm is assigned to the typical π-π* transition corresponding to the locally excited state.[39] The one-photon fluorescence (OPFL) of **N** was obtained with the excitation wavelength of 400 nm (Fig. 1), showing a single peak localizing at wavelength of 604 nm, indicating that the fluorescence emission occurs from the local excited state. The ICT singlet state mainly deactivates through a nonradiative decay to ICT triplet state via intersystem crossing.[23] The absorption maximum of **N** in chloroform appears at 328 nm, while the absorption maximum of **WI** in water is at 290 nm with a 38 nm hypsochromic shift compared with **N** due to the decreasing the polarity of the microenvironment around **N**.[40] Another possible reason is that O-H···O and C-H···O hydrogen bonds formed between 2-Hp-β-CDs and **N** result in the electron redistribution of **N** and increase the stability of **N** simultaneously.[41] There is only one peak at the wavelength of 527 nm in the fluorescence spectra of **WI**, which also has hypsochromic shift compared with **N**. The fluorescence quantum yield of samples in solutions were recorded with coumarin 307 (Φ=0.58) as a reference in acetonitrile. The Φ values of **N** and **WI** are listed in Table 1. The fluorescence quantum yield of **WI** (Φ=0.007) is lower compare with **N** (Φ=0.023).

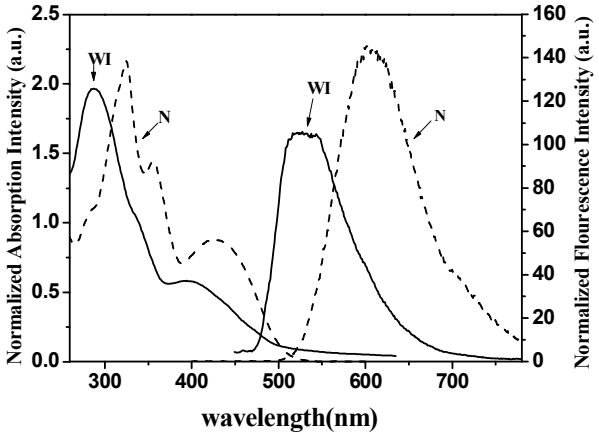

Fig. 1 Normalized UV-vis and fluorescence spectra of **WI** (solid line) and **N** (dashed line). The excitation wavelength for fluorescence measurement is 400 nm. **WI** and **N** are dissolved in H_2O and $CHCl_3$, respectively.

FTIR studies

FTIR spectroscopy was used to confirm the host-guest chemical interaction of **N** and 2-Hp-β-CDs. The FTIR spectra of **N** (A), 2-Hp-β-CDs (B), physical mixture of **N** and 2-Hp-β-CDs (C) as well as **WI** (D) are shown in Fig. 2. The spectrum of C is almost the superposition of A and B. Not only the characteristic carbonyl (1671 cm^{-1}), benzene (1592 cm^{-1}, 1510 cm^{-1}), and aromatic ether bond band (1256 cm^{-1}) of **N** can be found, but also the characteristic hydroxyl and alkyl band of 2-Hp-β-CDs.

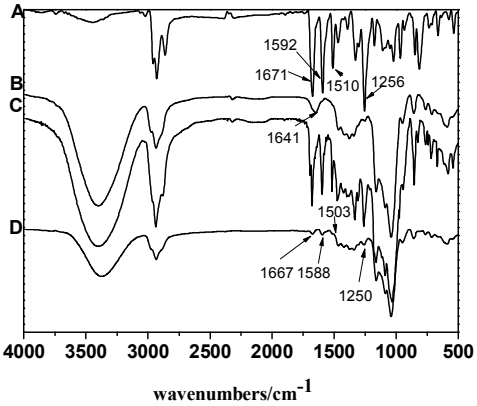

Fig. 2 FTIR spectra of N (A), 2-Hp-β-CDs (B), physical mixture of **N** and 2-Hp-β-CDs (C) and **WI** (D).

Although some peaks of **N**, e.g. at 1667 cm^{-1}, 1588 cm^{-1}, 1503 cm^{-1} and 1250 cm^{-1} still appear in spectrum D, the intensity of the corresponding four peaks of **WI** are found to decrease and even disappear because some functional groups of **N** are packed by 2-Hp-β-CDs completely. Meanwhile, the peak of 1641 cm^{-1} in D weakens and even disappears because of the formation of O-H···O and C-H···O hydrogen bonds between **N** and 2-HP-β-CDs.[42] The FTIR results demonstrated **N** and 2-HP-β-CDs

assembled with each other through host-guest chemical interaction rather than simple physical mixture.

NMR studies of N and inclusion complexes

The ^{1}H NMR spectra of 2-Hp-β-CDs (A), **N** (B) and **WI** (C) are shown in Fig. 3. Two resonance peaks at chemical shifts around 1.44 ppm (CH_3-C***H***$_2$-C***H***$_2$-CH_2-CH_2-) and 1.78 ppm (CH_3-$(CH_2)_2$-C***H***$_2$-CH_2-) are attributed to methylene protons belonging to the alkyl chain of **N** (shown in spectrum of C), which are not packed by 2-Hp-β-CDs and still exist in the ^{1}H NMR spectrum of **WI**. While the chemical shift of methyl protons (C***H***$_3$-$(CH_2)_3$-CH_2-) in **N** overlaps with those in 2-Hp-β-CDs. The chemical shift of methylene protons (CH_3-$(CH_2)_2$-C***H***$_2$-CH_2-) has a little change due to the influence of C-H···O hydrogen bond, which also shows micro-variation of chemical shifts due to the existence of 2-Hp-β-CDs. Meanwhile, the chemical shift of peak at around 8 ppm in C corresponding to phenyl protons of **N** disappears because the phenyls protons are packed by 2-Hp-β-CDs completely.[43] The ^{1}H NMR results also confirmed that **N** and 2-Hp-β-CDs assembled with each other through host-guest chemical interaction instead of simple physical blend.

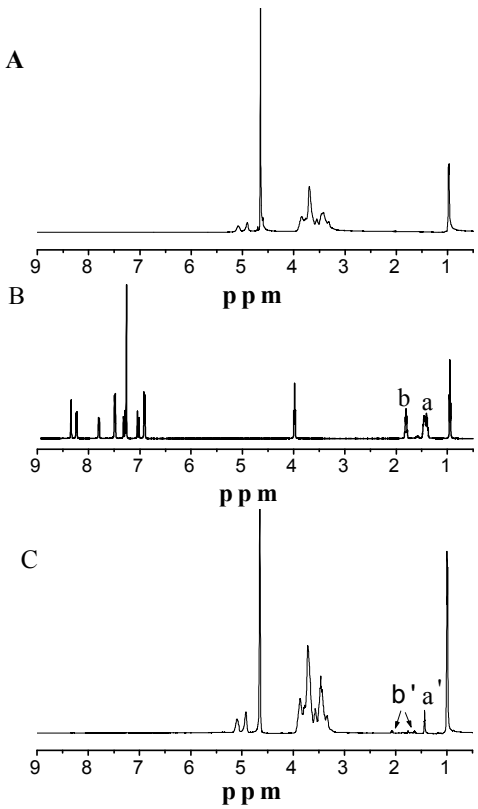

Fig. 3 ^{1}H NMR spectra (500 MHz) of 2-Hp-β-CDs (A), **N** (B) and **WI** (C).

Nonlinear optical properties

The TPA nonlinear relation and δ_{TPA} of **N** and **WI** are shown in Fig. 4A and Fig. 4B, respectively. Fig. 4A shows that the fluorescent integral area and laser energy of **N** and **WI** have a quadratic relationship, indicating that the absorption of **N** and **WI** is TPA process, a three order nonlinear optical effect. The δ_{TPA} values of **N** and **WI** are also listed in Table 1. **N** and **WI** have TPA cross-section maxima around 600 GM and 300 GM at the wavelength of 820 nm and 770 nm, respectively. In aqueous medium, the δ_{TPA} value of **WI** is around 200 GM at 780 nm that is much larger compared with those commercial initiators and most of water-soluble TPA materials reported with low δ_{TPA} value less than 100 GM.[37, 44] It is known that the TPA intensity is strongly dependent on intramolecular charger transfer (ICT).[21] Compared with **N**, the δ_{TPA} values of **WI** decreased probably due to the change of ICT of **N** in **WI**, in which **N** was restricted by 2-Hp-β-CDs through hydrogen bonds formed between O-H···O and C-H···O.[40]

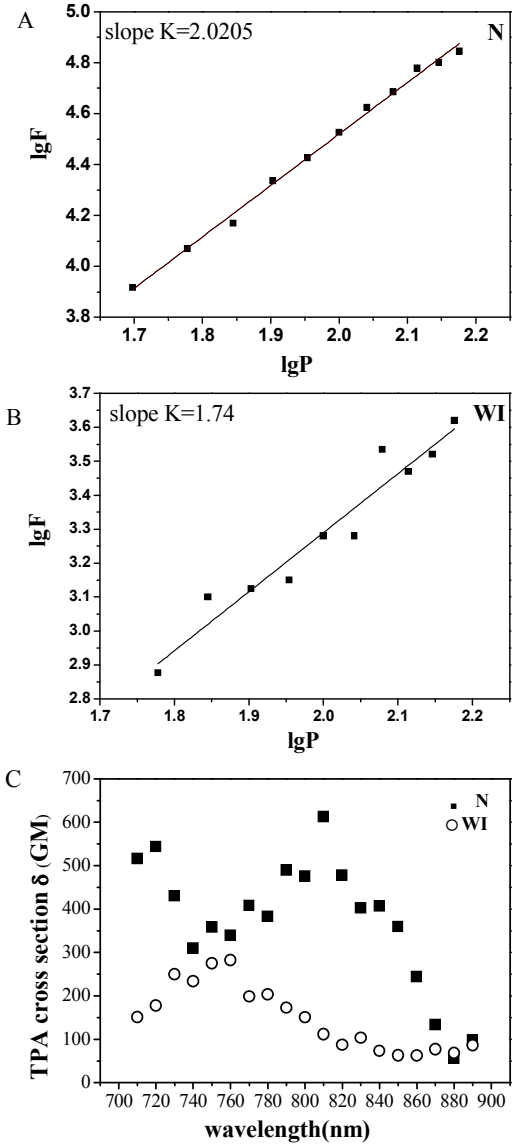

Fig. 4 The TPA nonlinear relation **N** (A), **WI** (B) and cross-section (C) of **N**, **WI** in range 710-890 nm. **N** and **WI** are dissolved in $CHCl_3$ and H_2O, respectively.

Table 1 Photophysical data of **N** and **WI** at room temperature

Compound	Solvent	λ_{abs}max/nm[a]	λ_{em}max/nm[b]	Φ_f[dc]	δ_{TPA}max[d]/GM
N	$CHCl_3$	327	611	0.023	612
WI	H_2O	290	527	0.007	282

[a] Peak wavelength of one-photon absorption. [b] Peak wavelength of one-photon fluorescence. [c] Fluorescence quantum yield determined relative to coumarin 307 (Φ=0.58 in acetonitrike). [d] The maximum of two-photon absorption cross-section. 1 GM=10^{-50} cm^4 s $photon^{-1}$.

3.5 Two-photon polymerization of 3D hydrogels

Threshold energy and scanning speed of TPP are two key parameters to evaluate initiating efficiency of a photoinitiator. The threshold energy of TPP is usually defined as the lowest average laser power which can produce the solid polymer lines from a photoresist resin.[45] In the previous report, microfabrication of 3D hydrogels via TPP needed high threshold energy due to the low initiating efficiency of photoinitiators.[33-35] PEGda has shown the feasibility for TPP of hydrogels.[38] In this work, PEGda (Mn = 700) was used as monomer to fabricate 3D hydrogels with woodpile structure. The threshold energy for **WI** at a linear scanning speed of 10 μm s^{-1} was 8.6 mW (the molar ratio of **N** in resin is 0.03%), and that was only 10.2 mW at the scanning speed as high as 50 μm s^{-1}. The SEM images on TPP results are shown in Fig. 5. The solid lines (Fig. 5 (A-C)) and 3D hydrogels with woodpile microstructure (Fig. 5 (D-F)) were fabricated by using average power of 9.7 mW with linear scanning speed of 30 μm s^{-1}. The smooth and continuous solid lines have been obtained. It shows that the width of fabricated lines are around 200 nm and the resolution is improved compared with that of the previously reported hydrogels fabricated by TPP.[34, 35] For example, the linewidth in Jhaveri's report was around 1 μm.[34] The 3D woodpile microstructure has been achieved and shows a regular structure and uniform clearance similar to cell scaffold with sizes fitting in a volume of 80 × 80 × 17 μm^3, demonstrating the potential of the photoresist to fabricate 3D scaffold for tissue engineering.

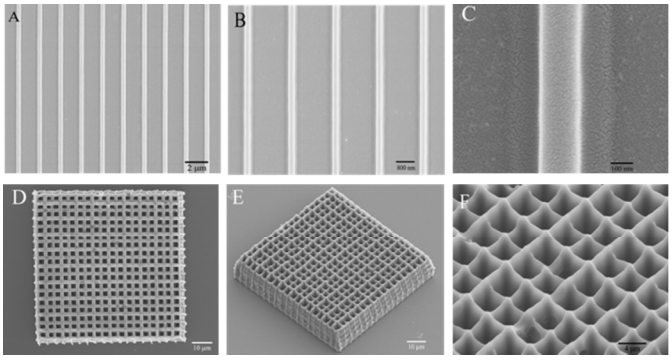

Fig. 5 The SEM images on TPP microfabrication. (A-C) show the solid polymer lines and (D-F) show 3D hydrogels with a woodpile structure with 80 × 80 × 17 μm^3.

Conclusions

A water soluble TPP initiator (**WI**) was successfully prepared by combining 2, 7-bis(2-(4-pentaneoxy-phenyl)-vinyl)anthraquinone with C_{2v} symmetrical structure and 2-hydroxypropyl-β-cyclodextrins through host-guest chemical interaction. The **WI** owned a large two-photon absorption cross-section of around 200 GM in aqueous medium. The threshold energy in two-photon polymerization for **WI** was 8.6 mW at a linear scanning speed of 10 μm s^{-1}, while it was 10.2 mW when the scanning speed was high up to 50 μm s^{-1}. The laser threshold energy for fabrication of 3D hydrogels was dramatically decreased and the resolution was largely improved. This work provides a green and facile method to fabricate 3D hydrogels via TPP in aqueous medium.

Acknowledgements

Authors thank the support of the National Natural Science Foundation of China (31371014, 61205194 and91123032), the National Natural Science Youth Foundation of China (31100722 and 51203111) and Tianjin Natural Science Foundation (13JCYBJC16500).

Notes

[a] *Department of Polymer Science and Engineering, School of Chemical Engineering and Technology, Tianjin University, Tianjin 300072, P. R. China.*

[b] *Laboratory of Organic NanoPhotonics and Key Laboratory of Functional Crystals and Laser Technology, Technical Institute of Physics and Chemistry, Chinese Academy of Sciences, No.29 Zhongguancun East Road, Beijing 100190, P. R. China.*

[c] *Chongqing Institute of Green and Intelligent Technology, Chinese Academy of Sciences, No.266 Fangzheng Ave, Shuitu technology development zone, Beibei District, Chongqing 400714, P. R. China. E-mail: jinfengxing@tju.edu.cn; zhengmeiling@mail.ipc.ac.cn; xmduan@mail.ipc.ac.cn*

References

1. W. Kaiser and C. Garrett, *Phy. Rev. Lett.*, 1961, **7**, 229-231.
2. A. M. Göppert-Mayer, *Ann. Phys.*, 1931, **9**, 273.
3. F. Terenziani, C. Katan, E. Badaeva, S. Tretiak and M. Blanchard-Desce, *Adv. Mater.*, 2008, **20**, 4641-4678.
4. W. Denk, J. H. Strickler and W. W. Webb, *Science*, 1990, **248**, 73-76.
5. M.-L. Zheng, K. Fujita, W.-Q. Chen, N. I. Smith, X.-M. Duan and S. Kawata, *ChemBioChem*, 2011, **12**, 52-55.
6. Y.-C. Zheng, M.-L. Zheng, S. Chen, Z.-S. Zhao and X.-M. Duan, *J. Mater. Chem. B*, 2014, **2**, 2301-2310.
7. S. Kawata, H.-B. Sun, T. Tanaka and K. Takada, *Nature*, 2001, **412**, 697-698.
8. S. Maruo, O. Nakamura and S. Kawata, *Opt. Lett.*, 1997, **22**, 132-134.
9. Z.-B. Sun, X.-Z. Dong, W.-Q. Chen, S. Nakanishi, X.-M. Duan and S. Kawata, *Adv. Mater.*, 2008, **20**, 914-919.
10. W.-K. Wang, Z.-B. Sun, M.-L. Zheng, X.-Z. Dong, Z.-S. Zhao and X.-M. Duan, *J. Phys. Chem. C*, 2011, **115**, 11275-11281.

11. D. A. Parthenopoulos and P. M. Rentzepis, *Science*, 1989, **245**, 843-845.
12. M. P. Joshi, J. Swiatkiewicz, F.-M. Xu and P. N. Prasad, *Opt. Lett.*, 1998, **23**, 1742-1744.
13. C. Fowley, N. Nomikou, A. P. McHale, P. A. McCarron, B. McCaughan and J. F. Callan, *J. Mater. Chem.*, 2012, **22**, 6456-6462.
14. M. Pawlicki, H. A. Collins, R. G. Denning and H. L. Anderson, *Angew. Chem. Int. Ed.*, 2009, **48**, 3244-3266.
15. B. H. Cumpston, S. P. Ananthavel, S. Barlow, D. L. Dyer, J. E. Ehrlich, L. L. Erskine, A. A. Heikal, S. M. Kuebler, I.-Y. Sandy Lee, D. McCord-Maughon, J.-Q Qin, H. Röckel, M. Rumi. X.-L. Wu, S. R. Marder and J. W. Perry, *Nature*, 1999, **398**, 51-54.
16. M. Farsari and B. N. Chichkov, *Nature Photonics*, 2009, **3**, 450-452.
17. J.-F. Xing, X.-Z. Dong, W.-Q. Chen, X.-M. Duan, N. Takeyasu, T. Tanaka and S. Kawata, *Appl. Phys. Lett.*, 2007, **90**, 131106.
18. C. D. Marco, A. Gaidukeviciute, R. Kiyan, S. M. Eaton, M. Levi, R. Osellame, B. N. Chichkov and S. Turri, *Langmuir*, 2013, **29**, 426-431.
19. H.-Z. Cao, M.-L. Zheng, X.-Z. Dong, F. Jin, Z.-S. Zhao and X.-M. Duan, *Appl. Phys. Express*, 2013, **6**, 066501.
20. C. N. LaFratta, J. T. Fourkas, T. Baldacchini and R. A. Farrer, *Angew. Chem. Int. Ed.*, 2007, **46**, 6238-6258.
21. M. Albota, D. Beljonne, J. L. Brédas, J. E. Ehrlich, J.-Y. Fu, A. A. Heikal, S. E. Hess, T. Kogej, M. D. Levin, S. R. Marder, D. McCord-Maughon, J. W. Perry, H. Röckel, M. Rumi, G. Subramaniam, W. W. Webb, X.-L. Wu and C. Xu, *Science*, 1998, **281**, 1653-1656.
22. E. Zojer, D. Beljonne, P. Pacher and J. L. Bredas, *Chem. Eur. J.*, 2004, **10**, 2668-2680.
23. J.-F. Xing, W.-Q. Chen, X.-Z. Dong, T. Tanaka, X.-Y. Fang, X.-M. Duan and S. Kawata, *J. Photochem. Photobiol. A*, 2007, **189**, 398-404.
24. J.-F. Xing, W.-Q. Chen, J. Gu, X.-Z. Dong, N. Takeyasu, T. Tanaka, X.-M. Duan and S. Kawata, *J. Mater. Chem. A*, 2007, **17**, 1433-1438.
25. Y. Ren, X.-Q. Yu, D.-J. Zhang, D. Wang, M.-L. Zhang, G.-B. Xu, X.-Z. Zhao, Y.-P. Tian, Z.-S, Shao and M.-H. Jiang, *J. Mater. Chem*., 2002, **12**, 3431-3437.
26. W.-E. Lu, X.-Z. Dong, W.-Q. Chen, Z.-S. Zhao and X.-M. Duan, *J. Mater. Chem.*, **2011**, *21*, 5650-5659.
27. X.-M. Wang, F. Jin, Z.-G. Chen, S.-Q. Liu, X.-H. Wang, X.-M. Duan, X.-T. Tao and M.-H. Jiang, *J. Phys. Chem. C*, 2011, **115**, 776-784.
28. J.-F. Xing, M.-L. Zheng, W.-Q. Chen, X.-Z. Dong, N. Takeyasu, T. Tanaka, Z.-S. Zhao, X.-M. Duan and S. Kawata, *Phys. Chem. Chem. Phys.*, 2012, **14**, 15785-15792.
29. N. A. Peppas, J. Z. Hilt, A. Khademhosseini and R. Langer, *Adv. Mater.*, 2006, **18**, 1345-1360.
30. D. Seliktar, *Science*, 2012, **336**, 1124-1128.
31. A. Ovsianikov, J. Viertl, B. Chichkov, M. Oubaha, B. MacCraith, I. Sakellari, A. Giakoumaki, D. Gray, M. Vamvakaki, M. Farsari and Costas Fotakis, *ACS Nano*, 2008, **2**, 2257-2262.
32. T. watanabe, M. Akiyama, K. Totani, S. M. Kuebler, F. Stallacci, W. Wenseleers, K. Braun, S. R. Marder and J. W. Perry, *Adv. Funct. Mater.*, 2002, **12**, 611-614.
33. Z. Xiong, M.-L. Zheng, X.-Z. Dong, W.-Q. Chen, F. Jin, Z.-S. Zhao and X.-M. Duan, *Soft Matter*, 2011, **7**, 10353-10359.
34. S. J. Jhaveri, J. D. Mcmullen, R. Sijbesma, L.-S. Tan, W. Zipfel and C. K. Ober, *Chem. Mater.*, 2009, **21**, 2003-2006.
35. J. Torgersen, A. Ovsianikov, V. Mironov, N. Pucher, X.-H. Qin, Z.-Q. Li, K. Cicha, T. Machacek, R. Liska, V. Jantsch and J. Stampfl, *J. Biomed. Opt.*, 2012, **17,** 105008.
36. I. Wang, M. Bouriau, P. L. Baldeck, C. Martineau and C. Andraud, *Opt. Lett.*, 2002, **27**, 1348-1350
37. Y. Tian, C. Y. Chen, Y. J. Cheng, A. C. Young, N. M. Tucker and A. K. Y. Jen, *Adv. Funct. Mater.*, 2007, **17**, 1691-1697.
38. J. Torgersen, X.-H. Qin, Z. Li, A. Ovsianikov, R. Liska and J. Stampfl, *Adv. Funct. Mater.*, 2013, **23**, 4542-4554.
39. D. Beljonne, J. L. Brédas, M. Cha, W. E. Torruellas, G. I. Stegeman, J. W. Hofstraat, W. H. G. Horsthuis and G. R. Mo□hlmann, *J. Chem. Phys.*, 1995, **103**, 7834-7843.
40. O. K. Nag, R. R. Nayak, C. S. Lim, I. H. Kim, K. Kyhm, B. R. Cho and H. Y. Woo, *J. Phys. Chem. B*, 2010, **114**, 9684-9690.
41. W. Saenger and T. Steiner, *Acta Crystallogr, Sect. A*, 1998, **54**, 798-805.
42. S. Das, M. T. Joseph and D. Sarkar, *Langmuir*, 2013, **29**, 1818-1830.
43. J.-Y. Tsao, C.-P. Wu, H.-H. Tsai, K.-C. Peng, P.-Y. Lin, S.-Y. Su, L.-D. Chen, F.-J. Tsai and Y. Tsai, *J. Incl. Phenom. Macrocycl. Chem.*, 2011, **72**, 405-411.
44. C. Xu and W. W. Webb, *J. Opt. Soc. Am. B*, 1996, **13**, 481-491.
45. Y. Ren, X.-Q. Yu, D.-J. Zhang, D. Wang, M.-L. Zhang, G.-B. Xu, X. Zhao, Y.-P. Tian, Z.-S. Shao and M.-H. Jiang, *J. Mater. Chem.*, 2002, **12**, 3431-3437.